Available online at www.sciencedirect.com
SCIENCE DIRECT®
Journal of Solid State Chemistry 176 (2003) 159–164
JOURNAL OF SOLID STATE CHEMISTRY
http://elsevier.com/locate/jssc

Hydrothermal synthesis and crystal structure of a three-dimensional vanadium tellurite $V_4Te_4O_{18}$

Dongrong Xiao, Shutao Wang, Enbo Wang,* Yu Hou, Yangguang Li, Changwen Hu, and Lin Xu

Department of Chemistry, Institute of Polyoxometalate Chemistry, Northeast Normal University, Changchun, Jilin 130024, People's Republic of China

Received 9 April 2003; received in revised form 20 June 2003; accepted 3 July 2003

Abstract

A novel vanadium tellurite $V_4Te_4O_{18}$ was synthesized by the hydrothermal reaction of V_2O_5, Na_2TeO_3, $CuCl_2 \cdot 6H_2O$, and water. Its structure was determined by elemental analyses, XPS spectra, TG analysis, IR spectrum and the single-crystal X-ray diffraction. The title compound crystallizes in monoclinic system, space group $P2(1)/c$, $a = 7.2475(14)$ Å, $b = 9.4901(19)$ Å, $c = 10.073(2)$ Å, $\beta = 94.45(3)°$, $V = 690.7(2)$ Å^3, $Z = 2$, $\lambda(\text{Mo}K\alpha) = 0.71073$ Å, ($R(F) = 0.0316$ for 1580 reflections). Data were collected on a Rigaku R-AXIS RAPID IP diffractometer at 293 K in the range of $2.82 < \theta < 27.47°$. The title compound exhibits a novel three-dimensional (3D) framework, formed by VO_6 octahedra, VO_5 square pyramids, TeO_4 folded squares, and TeO_5 square pyramids via the corner- and/or edge-sharing mode. The 3D framework consists of two different types of one-dimensional (1D) tunnels parallel to *a*-axes.

Keywords: Vanadium tellurite; Three-dimensional framework; Hydrothermal synthesis; Crystal structure

1. Introduction

Tellurium oxides are of remarkable importance for their special applications in semi-conductive and optical materials [1–9]. Recent interests in vanadium tellurite glasses have stemmed from their large third-order non-linear susceptibility [1,2], high infrared transmittance [3], semi-conducting properties [4], and their potential uses as solid-state electrolytes [5,6].

Traditionally, tellurium oxides containing a dense packing of atoms have been prepared in glass form by high-temperature solid-state reactions [10]. Besides their high-energy consumption, these high-temperature solid state reactions involve a series of laborious heating cycles at high temperatures and repeated grinding of starting oxide components. The resulting glasses are amorphous and compositionally inhomogeneity. However, particular morphology and compositionally homogeneity of the tellurium oxides are crucial in terms of electrical and optical applications. Thus there is a real need to develop an alternative synthesis route for tellurium oxides. In the recent years, a lot of examples have powerfully testified that hydrothermal and/or nonaqueous solvothermal synthesis [11–13] is a highly effective route to single crystals of new, condensed, anhydrous materials, including tellurites. Crystal structures containing Te^{4+} are of interest because tellurium in the +4 oxidation state is known to exhibit a variety of coordination geometry structures [14–17], such as TeO_3 trigonal pyramids, TeO_4 folded squares, and TeO_5 with square pyramidal geometry, which could lead to a rich structural chemistry. Moreover, since vanadium can also adopt several kind of coordination modes [13], it can be presumed that novel V–Te–O frameworks be explored by incorporating tellurium and vanadium into a single structure. Furthermore, crystalline vanadium tellurite compounds may assist in understanding the properties and structures of important vanadium tellurite glasses by rationalizing the connectivity patterns for the V/O and Te/O units [18–20]. Thus, the preparation of novel vanadium tellurites has an intriguing perspective.

In this paper, we report the hydrothermal synthesis and crystal structure of a novel vanadium tellurite $V_4Te_4O_{18}$. The title compound exhibits a novel

*Corresponding author. Fax: +86-431-568-4009.
E-mail address: wangenbo@public.cc.jl.cn (E. Wang).

0022-4596/$ - see front matter © 2003 Elsevier Inc. All rights reserved.
doi:10.1016/S0022-4596(03)00381-5

three-dimensional (3D) scaffolding which contains two different types of one-dimensional (1D) tunnels parallel to *a*-axes.

2. Experimental section

2.1. General procedures

All chemicals were commercially purchased and used without further purification. V and Te were determined by a PLASMA-SPEC(I) ICP atomic emission spectrometer. XPS analyses were performed on a VG ESCALABMK II spectrometer with an Mg$K\alpha$ (1253.6 eV) achromatic X-ray source. The vacuum inside the analysis chamber was maintained at 6.2×10^{-6} Pa during the analysis. IR spectra was recorded in the range 400–4000 cm^{-1} on an Alpha Centaurt FT/IR spectrophotometer using KBr pellets. TG analysis was performed on a Perkin-Elmer TGA7 instrument in flowing N_2 with a heating rate of 10°C min^{-1}.

2.2. Hydrothermal synthesis

The title compound was hydrothermally synthesized under autogenous pressure. A mixture of $CuCl_2\cdot2H_2O$ (0.0426 g), V_2O_5 (0.0909 g), Na_2TeO_3 (0.2216 g), and H_2O (9 mL) in a molar ratio of 1:2:4:2000 was stirred for 30 min in air. The mixture was sealed in a 18 mL Teflon-lined autoclave and heated at 170°C for 144 h. Then the autoclave was cooled at 10°C h^{-1} to room temperature. Pink block crystals of $V_4Te_4O_{18}$ were isolated from a mixture of $V_4Te_4O_{18}$ and an unidentified black solid. The yield of $V_4Te_4O_{18}$ was ca. 70% based on vanadium. $CuCl_2\cdot2H_2O$ is necessary for this reaction though copper is not incorporated into the structure of the title compound. The pink crystals were manually selected for structural determination and further characterization. Elemental analyses results of the pink crystals are consistent with the stoichiometry of $V_4Te_4O_{18}$. Calc. for $V_4Te_4O_{18}$: Te, 50.7; V, 20.2%. Found: Te, 50.9; V,

Table 1
Crystal data and structure refinement for $V_4Te_4O_{18}$

Empirical formula	$O_{18}Te_4V_4$
Formula weight	1002.16
Temperature	293(2) K
Wavelength	0.71073 Å
Crystal system	Monoclinic
Space group	*P*2(1)/*c*
Unit cell dimensions	$a = 7.2475(14)$ Å, $\alpha = 90°$
	$b = 9.4901(19)$ Å, $\beta = 94.45(3)°$
	$c = 10.073(2)$ Å, $\gamma = 90°$
Volume	690.7(2) Å^3
Z	2
D_{cal}	4.819 mg/m^3
Absorption coefficient	11.010 mm^{-1}
θ range for data collection	2.82–27.47°
Reflections collected	2931
Independent reflections	1580 [$R_{(int)} = 0.0217$]
Data/restraints/parameters	1580/0/118
Final *R* indices [$I > 2\sigma(I)$]	$R_1 = 0.0316, wR_2 = 0.0868$
R indices (all data)	$R_1 = 0.0370, wR_2 = 0.0878$

Table 2
Selected bond lengths (Å) and angles (deg) for $V_4Te_4O_{18}$

Te(1)–O(2)	1.894(4)	Te(1)–O(6)#1	2.427(5)
Te(1)–O(3)	1.921(4)	Te(1)–O(4)	2.439(4)
Te(1)–O(1)	1.975(4)	Te(2)–O(4)	1.868(4)
Te(2)–O(8)	1.889(4)	Te(2)–O(2)#3	2.435(4)
Te(2)–O(5)#2	1.967(4)	V(1)–O(9)	1.584(5)
V(1)–O(5)	1.788(4)	V(1)–O(3)	1.897(4)
V(1)–O(8)#1	1.880(4)	V(1)–O(1)	2.002(4)
V(2)–O(7)	1.602(5)	V(2)–O(2)#3	1.979(4)
V(2)–O(6)	1.719(4)	V(2)–O(4)	2.025(4)
V(2)–O(1)	1.974(4)	V(2)–O(3)#4	2.304(4)
O(2)–Te(1)–O(3)	99.81(18)	O(1)–Te(1)–O(6)#1	142.13(16)
O(2)–Te(1)–O(1)	92.19(18)	O(2)–Te(1)–O(4)	91.27(17)
O(3)–Te(1)–O(1)	74.88(17)	O(3)–Te(1)–O(4)	139.63(16)
O(2)–Te(1)–O(6)#1	82.59(17)	O(1)–Te(1)–O(4)	65.95(15)
O(3)–Te(1)–O(6)#1	69.21(16)	O(6)#1–Te(1)–O(4)	151.12(14)
O(4)–Te(2)–O(8)	101.08(19)	O(4)–Te(2)–O(2)#3	69.72(16)
O(4)–Te(2)–O(5)#2	86.98(18)	O(8)–Te(2)–O(2)#3	85.97(17)
O(8)–Te(2)–O(5)#2	90.69(19)	O(5)#2–Te(2)–O(2)#3	155.27(16)
O(9)–V(1)–O(5)	104.0(2)	O(8)#1–V(1)–O(3)	88.06(19)
O(9)–V(1)–O(8)#1	102.9(2)	O(9)–V(1)–O(1)	101.3(2)
O(5)–V(1)–O(8)#1	97.1(2)	O(5)–V(1)–O(1)	86.64(19)
O(9)–V(1)–O(3)	108.5(2)	O(8)#1–V(1)–O(1)	153.75(19)
O(5)–V(1)–O(3)	145.0(2)	O(3)–V(1)–O(1)	74.77(18)
O(7)–V(2)–O(6)	102.8(2)	O(6)–V(2)–O(4)	148.3(2)
O(7)–V(2)–O(1)	96.6(2)	O(1)–V(2)–O(4)	74.95(17)
O(6)–V(2)–O(1)	93.5(2)	O(2)#3–V(2)–O(4)	77.35(17)
O(7)–V(2)–O(2)#3	96.2(2)	O(7)–V(2)–O(3)#4	172.8(2)
O(6)–V(2)–O(2)#3	107.8(2)	O(6)–V(2)–O(3)#4	75.44(18)
O(1)–V(2)–O(2)#3	151.91(18)	O(1)–V(2)–O(3)#4	90.50(17)
O(7)–V(2)–O(4)	107.8(2)	O(2)#3–V(2)–O(3)#4	77.93(17)
O(4)–V(2)–O(3)#4	75.20(17)		

Symmetry transformations used to generate equivalent atoms: #1 $-x$, $y-1/2$, $-z+3/2$; #2 $x+1$, y, z; #3 x, $-y+1/2$, $z-1/2$; #4 $-x$, $y+1/2$, $-z+3/2$; #5 x, $-y+1/2$, $z+1/2$; #6 $x-1$, y, z.

Table 3
Atomic coordinates ($\times10^4$) and equivalent isotropic displacement parameters (Å$^2\times10^3$) for $V_4Te_4O_{18}$

	x	*y*	*z*	$U_{(eq)}$
Te(1)	1382(1)	244(1)	7857(1)	7(1)
Te(2)	4570(1)	2794(1)	5643(1)	8(1)
V(1)	−2882(1)	423(1)	7419(1)	8(1)
V(2)	12(1)	2499(1)	5376(1)	7(1)
O(1)	−585(6)	1429(5)	6968(4)	9(1)
O(2)	1784(6)	1537(5)	9283(4)	9(1)
O(3)	−900(6)	−591(5)	8314(4)	9(1)
O(4)	2494(6)	1947(5)	6290(4)	10(1)
O(5)	−4018(6)	2093(5)	7254(4)	11(1)
O(6)	−1942(6)	3526(5)	5372(5)	13(1)
O(7)	−587(7)	1301(5)	4309(4)	16(1)
O(8)	4460(6)	4611(5)	6398(4)	11(1)
O(9)	−3465(7)	−352(5)	6058(5)	17(1)

$U_{(eq)}$ is defined as one-third of the trace of the orthogonalized U_{ij} tensor.

20.3%. FT/IR data (cm^{-1}): 3443(bh), 997(m), 943(s), 797(s), 696(s), 669(s), 525(s), 493(m), 446(s), 421(m).

2.3. *X-ray crystallography*

The structure of $V_4Te_4O_{18}$ was determined by single-crystal X-ray diffraction. Crystallographic data are as follows: $V_4Te_4O_{18}$, monoclinic, $P2(1)/c$, $a = 7.2475(14)$ Å, $b = 9.4901(19)$ Å, $c = 10.073(2)$ Å, $\beta = 94.45(3)°$, $V = 690.7(2)$ Å^3, $Z = 2$, $D_{cal} = 4.819$, $\lambda(\text{Mo}K\alpha) = 0.71073$ Å. A pink single crystal of $V_4Te_4O_{18}$ ($0.378 \times 0.276 \times 0.234$ mm) was mounted on a glass fiber. Data were collected on a Rigaku R-AXIS RAPID IP diffractometer. Empirical absorption correction (ψ scan) was applied. The structure was solved by the direct method and refined by the Full-matrix least squares on F^2 using the SHELXTL-97 software [22]. All of the atoms were refined anisotropically. A total of 2931 (1580 unique, $R_{int} = 0.0217$) reflections were measured. Structure solution and refinement based on 1580 independent reflections with $I > 2\sigma(I)$ and 118 parameters gave $R_1(wR_2) = 0.0316(0.0868)\{R_1 = \sum||F_o| - |F_c||/\sum|F_o|;\ wR_2 = \sum[w(F_o^2 - F_c^2)^2]/\sum[w(F_o^2)^2]^{1/2}\}$. A summary of crystal data and structure refinement for $V_4Te_4O_{18}$ is provided in Table 1. The selected bond lengths and angles are listed in Table 2. The atomic coordinates and equivalent isotropic displacement parameters for $V_4Te_4O_{18}$ are given in Table 3 (CSD reference number 412924).

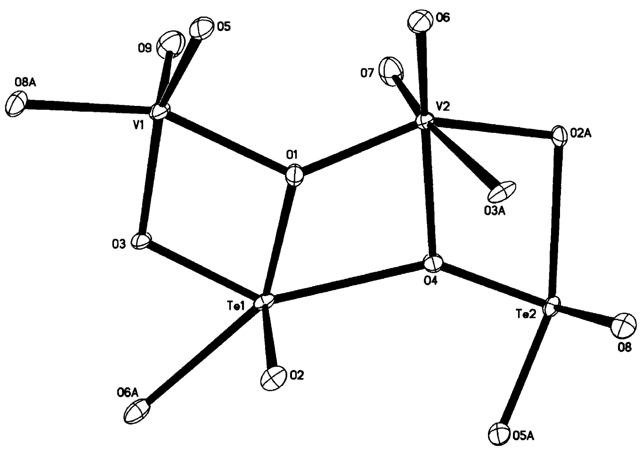

Fig. 1. View of the coordination environments of the vanadium and tellurium atoms, showing the atom-labeling scheme and 50% thermal ellipsoids.

3. Results and discussion

The single-crystal X-ray diffraction analysis reveals that $V_4Te_4O_{18}$ exhibits a novel 3D framework, formed

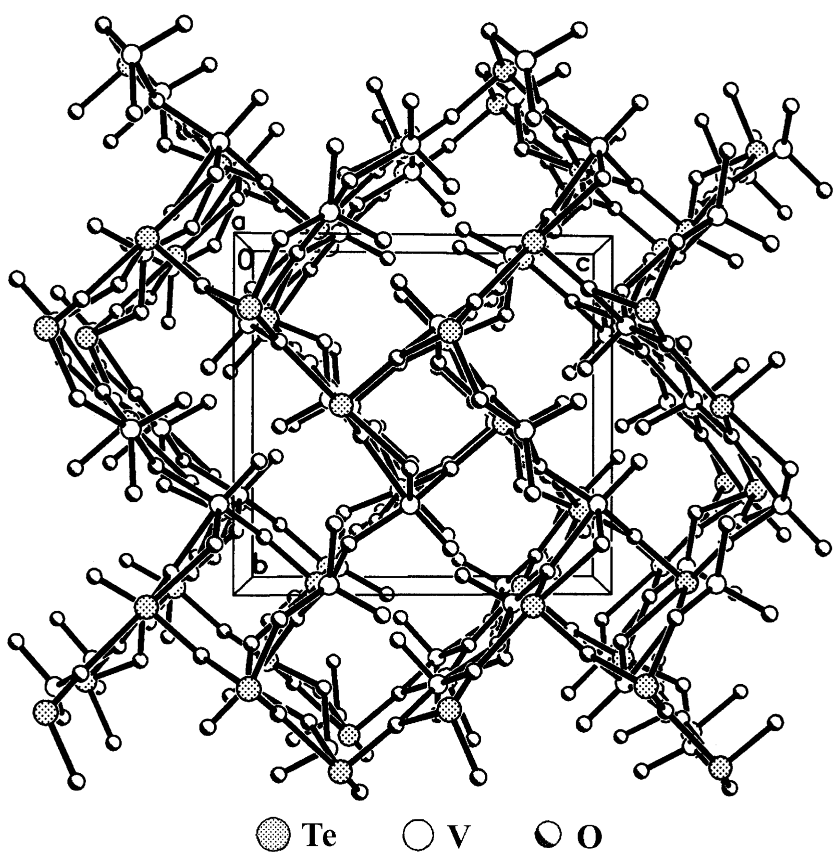

Fig. 2. View of the 3D structure of $V_4Te_4O_{18}$ along the *a*-axis direction.

by VO_6 octahedra, VO_5 square pyramids, TeO_4 folded squares, and TeO_5 square pyramids via the corner- and/or edge-sharing mode. The asymmetric unit of $V_4Te_4O_{18}$ (Fig. 1) shows the coordination environment around the vanadium and tellurium atoms. There are two crystallographically independent V atoms and two crystallographically independent Te atoms in this structure. The V(1) site exhibits a distorted square pyramidal coordination geometry with a terminal oxygen, two μ_2–O atoms linked with Te(2), and two μ_3–O atoms which are linked with V(2) and Te(1). The V(2) atom shows octahedral environment with a terminal oxygen, two μ_2–O atoms shared with Te(1) atom, and three μ_3–O atoms, two of which are linked with V(1) and Te(1), another linked with Te(1) and Te(2). The V–O bond lengths are in the range of 1.584(5) ~ 2.304(4) Å and the O–V–O angles 74.77(18) ~ 172.8(2)°. The Te(1) atom is square pyramidal coordination geometry with one μ_2–O atom bridging V(2) atom and four μ_3–O atoms, two of which are linked with V(2) and Te(2), the others linked with V(1) and V(2). As to the $Te(2)O_4$ folded square, two of the oxygen atoms bridge two V(1) atoms and the other two oxygen atoms are linked with Te(1) and V(2). The geometry of TeO_4 can be explained by VSEPR theory as an AX_4E trigonal bipyramid, with the lone pair occupying an equatorial position [20,21]. The Te–O bond lengths vary from 1.868(4) to 2.439(4) Å. The O–Te–O angles are in the range of 65.95(15)–155.27(16)°.

As shown in Fig. 1, the $V(1)O_5$ square pyramid and $Te(1)O_5$ square pyramid share an edge to give rise to a $V(1)Te(1)O_8$ moiety. The $V(2)O_6$ octahedron and the TeO_4 folded square link together via edge-sharing to form a $V(2)Te(2)O_8$ moiety. These two moieties are hold together by edge sharing to produce a $\{V_2Te_2O_{14}\}$ unit. Each $\{V_2Te_2O_{14}\}$ unit is linked with four adjacent $\{V_2Te_2O_{14}\}$ units through corner- and/or edge-sharing to form a two-dimensional (2D) network (Fig. 3). All 2D networks are parallel to *bc* plane and adjacent 2D networks are connected together by V(1)–O(5)–Te(2) bond to produce 3D framework (Figs. 2 and 3). The 3D framework contains two different types of rectangular tunnels parallel to *a*-axes. It is noteworthy that the coordination modes of Te^{4+} are very interesting. To best of our knowledge, only a few examples of tellurites contain Te^{4+} in two different coordination modes [12,16,20,24–26]. The title compound also contains Te^{4+} in two types of coordination modes, but in a rare combination of square pyramidal TeO_5 and folded square TeO_4.

The bond valence sum calculations [23] give the values of 5.02, and 5.03 for V(1), and V(2), showing that all V sites are in the +5 oxidation state. What's more, the calculations show the value of 4.00, and 3.93 for Te(1), and Te(2), indicating that all Te sites are in the +4 oxidation state. To confirm the calculated results, XPS spectra of $V_4Te_4O_{18}$ were also studied. The X-ray photoelectron spectrum (XPS) measurements of $V_4Te_4O_{18}$ in the energy regions of V_{2p} and Te_{3d} show peaks at 516.5 and 575.9 eV, attributable to V^{5+} and Te^{4+}, respectively (see Fig. 4). These results further confirm the valences of V and Te atoms.

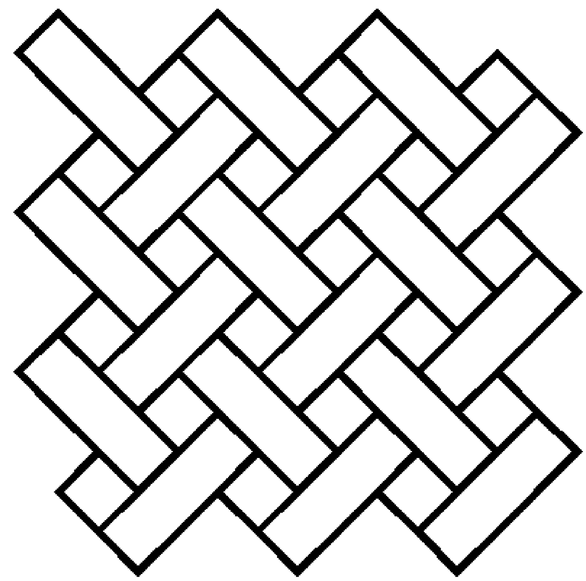

Fig. 3. Schematic illustration of the 2D networks that can be viewed as long-and-short brick.

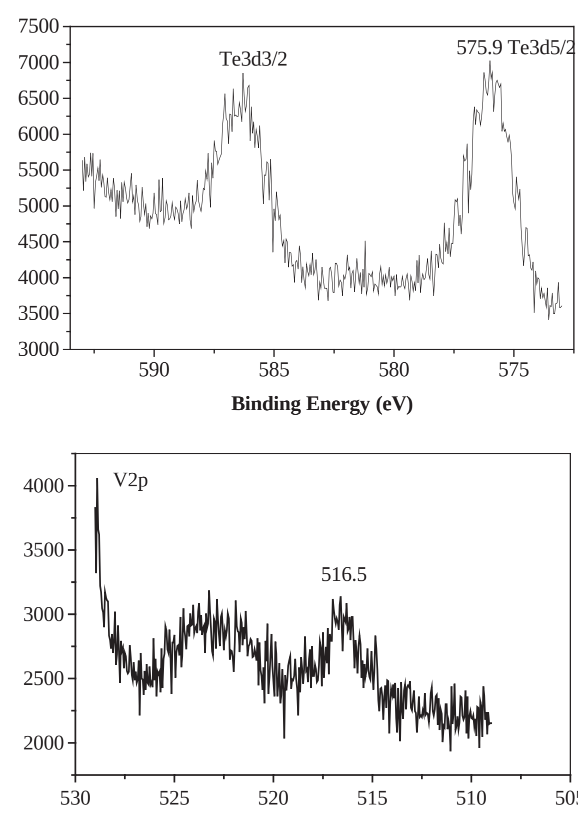

Fig. 4. X-ray photoelectron spectra (XPS) of $V_4Te_4O_{18}$.

In the infrared spectrum of $V_4Te_4O_{18}$, the strong bands at 997, 943, and 797 cm^{-1} could be assigned to the υ (V=O) or υ (V–O–V) vibrations. The peaks around 696, 669, 525 cm^{-1} in the infrared spectrum of $V_4Te_4O_{18}$ could be ascribed to one or more of the vibrations of V–O, Te–O, Te–O–V, all of which fall in this range.

Thermogravimetric analysis of $V_4Te_4O_{18}$ shows no weight loss until 600°C. The weight loss stating from 600°C should only be due to the loss of volatile component oxides.

In conclusion, we have prepared a novel 3D vanadium tellurite $V_4Te_4O_{18}$ consisting of two different types of rectangular tunnels parallel to *a*-axes. This work is a good example of the preparation of new tellurites with novel structural features by hydrothermal techniques, in the form of single crystals, enabling unambiguous structural characterization.

Acknowledgments

This work was financially supported by the National Science Foundation of China (20171010).

Appendix

See supplement tables (Tables S1–S4).

Table S1
Crystal data and structure refinement for $V_4Te_4O_{18}$

Empirical formula	$O_{18}Te_4V_4$
Formula weight	1002.16
Temperature	293(2) K
Wavelength	0.71073 Å
Crystal system	Monoclinic
Space group	$P2(1)/c$
Unit cell dimensions	$a = 7.2475(14)$ Å, $\alpha = 90°$
	$b = 9.4901(19)$ Å, $\beta = 94.45(3)°$
	$c = 10.073(2)$ Å, $\gamma = 90°$
Volume	690.7(2) $Å^3$
Z	2
D_{cal}	4.819 mg/m^3
Absorption coefficient	11.010 mm^{-1}
$F(000)$	888
Crystal size	$0.378 \times 0.276 \times 0.234\ mm^3$
θ range for data collection	2.82–27.47°
Limiting indices	$-9 \leqslant h \leqslant 9$, $-12 \leqslant k \leqslant 12$, $-13 \leqslant l \leqslant 13$
Reflections collected	2931
Independent reflections	1580 [$R_{(int)} = 0.0217$]
Completeness to $\theta = 27.47°$	99.8%
Absorption correction	Empirical
Refinement method	Full-matrix least-squares on F^2
Data/restraints/parameters	1580/0/118
Goodness-of-fit on F^2	1.023
Final R indices [$I > 2\sigma(I)$]	$R_1 = 0.0316$, $wR_2 = 0.0868$
R indices (all data)	$R_1 = 0.0370$, $wR_2 = 0.0878$
Largest diffraction peak and hole	1.210 and –2.3 $eÅ^{-3}$

Table S2
Atomic coordinates ($\times 10^4$) and equivalent isotropic displacement parameters ($Å^2 \times 10^3$) for $V_4Te_4O_{18}$

	x	y	z	$U_{(eq)}$
Te(1)	1382(1)	244(1)	7857(1)	7(1)
Te(2)	4570(1)	2794(1)	5643(1)	8(1)
V(1)	−2882(1)	423(1)	7419(1)	8(1)
V(2)	12(1)	2499(1)	5376(1)	7(1)
O(1)	−585(6)	1429(5)	6968(4)	9(1)
O(2)	1784(6)	1537(5)	9283(4)	9(1)
O(3)	−900(6)	−591(5)	8314(4)	9(1)
O(4)	2494(6)	1947(5)	6290(4)	10(1)
O(5)	−4018(6)	2093(5)	7254(4)	11(1)
O(6)	−1942(6)	3526(5)	5372(5)	13(1)
O(7)	−587(7)	1301(5)	4309(4)	16(1)
O(8)	4460(6)	4611(5)	6398(4)	11(1)
O(9)	−3465(7)	−352(5)	6058(5)	17(1)

$U_{(eq)}$ is defined as one-third of the trace of the orthogonalized U_{ij} tensor.

Table S3
Bond lengths (Å) and angles (deg) for $V_4Te_4O_{18}$

Te(1)–O(2)	1.894(4)	Te(1)–O(6)#1	2.427(5)
Te(1)–O(3)	1.921(4)	Te(1)–O(4)	2.439(4)
Te(1)–O(1)	1.975(4)	Te(2)–O(4)	1.868(4)
Te(2)–O(8)	1.889(4)	Te(2)–O(2)#3	2.435(4)
Te(2)–O(5)#2	1.967(4)	V(1)–O(9)	1.584(5)
V(1)–O(5)	1.788(4)	V(1)–O(3)	1.897(4)
V(1)–O(8)#1	1.880(4)	V(1)–O(1)	2.002(4)
V(2)–O(7)	1.602(5)	V(2)–O(2)#3	1.979(4)
V(2)–O(6)	1.719(4)	V(2)–O(4)	2.025(4)
V(2)–O(1)	1.974(4)	V(2)–O(3)#4	2.304(4)
O(2)–V(2)#5	1.979(4)	O(3)–V(2)#1	2.304(4)
O(2)–Te(2)#5	2.435(4)	O(5)–Te(2)#6	1.967(4)
O(8)–V(1)#4	1.880(4)	O(6)–Te(1)#4	2.427(5)
O(2)–Te(1)–O(3)	99.81(18)	O(1)–Te(1)–O(6)#1	142.13(16)
O(2)–Te(1)–O(1)	92.19(18)	O(2)–Te(1)–O(4)	91.27(17)
O(3)–Te(1)–O(1)	74.88(17)	O(3)–Te(1)–O(4)	139.63(16)
O(2)–Te(1)–O(6)#1	82.59(17)	O(1)–Te(1)–O(4)	65.95(15)
O(3)–Te(1)–O(6)#1	69.21(16)	O(6)#1–Te(1)–O(4)	151.12(14)
O(4)–Te(2)–O(8)	101.08(19)	O(4)–Te(2)–O(2)#3	69.72(16)
O(4)–Te(2)–O(5)#2	86.98(18)	O(8)–Te(2)–O(2)#3	85.97(17)
O(8)–Te(2)–O(5)#2	90.69(19)	O(5)#2–Te(2)–O(2)#3	155.27(16)
O(9)–V(1)–O(5)	104.0(2)	O(8)#1–V(1)–O(3)	88.06(19)
O(9)–V(1)–O(8)#1	102.9(2)	O(9)–V(1)–O(1)	101.3(2)
O(5)–V(1)–O(8)#1	97.1(2)	O(5)–V(1)–O(1)	86.64(19)
O(9)–V(1)–O(3)	108.5(2)	O(8)#1–V(1)–O(1)	153.75(19)
O(5)–V(1)–O(3)	145.0(2)	O(3)–V(1)–O(1)	74.77(18)
O(7)–V(2)–O(6)	102.8(2)	O(6)–V(2)–O(4)	148.3(2)
O(7)–V(2)–O(1)	96.6(2)	O(1)–V(2)–O(4)	74.95(17)
O(6)–V(2)–O(1)	93.5(2)	O(2)#3–V(2)–O(4)	77.35(17)
O(7)–V(2)–O(2)#3	96.2(2)	O(7)–V(2)–O(3)#4	172.8(2)
O(6)–V(2)–O(2)#3	107.8(2)	O(6)–V(2)–O(3)#4	75.44(18)
O(1)–V(2)–O(2)#3	151.91(18)	O(1)–V(2)–O(3)#4	90.50(17)
O(7)–V(2)–O(4)	107.8(2)	O(2)#3–V(2)–O(3)#4	77.93(17)
O(4)–V(2)–O(3)#4	75.20(17)	V(2)–O(1)–Te(1)	117.7(2)
V(2)–O(1)–V(1)	131.9(2)	Te(1)–O(1)–V(1)	102.07(19)
Te(1)–O(2)–V(2)#5	130.8(2)	Te(1)–O(2)–Te(2)#5	131.9(2)
V(2)#5–O(2)–Te(2)#5	96.44(16)	V(2)–O(4)–Te(1)	98.00(17)
V(1)–O(3)–Te(1)	108.1(2)	V(1)–O(5)–Te(2)#6	125.6(2)
V(1)–O(3)–V(2)#1	147.0(2)	V(2)–O(6)–Te(1)#4	106.8(2)
Te(1)–O(3)–V(2)#1	104.73(18)	V(1)#4–O(8)–Te(2)	132.6(2)
Te(2)–O(4)–V(2)	116.1(2)	Te(2)–O(4)–Te(1)	145.8(2)

Symmetry transformations used to generate equivalent atoms: #1 $-x$, $y-1/2$, $-z+3/2$; #2 $x+1$, y, z; #3 x, $-y+1/2$, $z-1/2$; #4 $-x$, $y+1/2$, $-z+3/2$; #5 x, $-y+1/2$, $z+1/2$; #6 $x-1$, y, z.

Table S4
Anisotropic displacement parameters ($Å^2 \times 10^3$) for $V_4Te_4O_{18}$

	U_{11}	U_{22}	U_{33}	U_{23}	U_{13}	U_{12}
Te(1)	5(1)	8(1)	8(1)	−2(1)	0(1)	0(1)
Te(2)	6(1)	7(1)	10(1)	−1(1)	2(1)	0(1)
V(1)	5(1)	8(1)	10(1)	0(1)	0(1)	1(1)
V(2)	6(1)	7(1)	9(1)	1(1)	0(1)	0(1)
O(1)	8(2)	9(2)	11(2)	3(2)	2(2)	0(2)
O(2)	7(2)	10(2)	10(2)	−5(2)	3(1)	1(2)
O(3)	5(2)	9(2)	14(2)	5(2)	−1(2)	0(2)
O(4)	5(2)	12(2)	14(2)	5(2)	1(2)	2(2)
O(5)	6(2)	11(2)	15(2)	3(2)	2(2)	2(2)
O(6)	9(2)	7(2)	22(2)	3(2)	−1(2)	2(2)
O(7)	21(2)	16(2)	11(2)	0(2)	2(2)	−3(2)
O(8)	8(2)	9(2)	15(2)	−1(2)	2(2)	2(2)
O(9)	14(2)	21(2)	15(2)	−3(2)	1(2)	−3(2)

The anisotropic displacement factor exponent takes the form: $-2pi^2[h^2a*^2\, U_{11} + \cdots + 2hka*b*U_{12}]$.

References

[1] H. Nasu, O. Matsushita, K. Kamiya, H. Kobayashi, K. Kubodera, J. Non-Cryst. Solids 124 (1990) 275–277.
[2] S. Kim, H.T. Yoko, S. Sakka, J. Am. Cream. Soc. 76 (1993) 2486.
[3] H. Burger, W. Vogel, V. Kozhukharov, Infrared Phys. 25 (1985) 395–409.
[4] M.A. Sidkey, A.A. El-Moneim, L.A. El-Latif, Mater. Chem. Phys. 61 (1999) 103–109.
[5] J. Rossognol, M. Reau, B. Tanguy, J. Videau, J. Porrtier, J. Non-Cryst. Solids 162 (1993) 244–252.
[6] D. Bersani, G. Antonioli, P.P. Lottci, Y. Dimitriev, V. Dimitrov, P. Kobourova, J. Non-Cryst. Solids 232–234 (1998) 293–299.
[7] S. Tanabe, K. Hirao, N. Soga, J. Non-Cryst. Solids 122 (1990) 79–82.
[8] H. Yusuke, A. Osaka, T. Nanba, Y. Miura, J. Non-Cryst. Solids 177 (1994) 164–169.
[9] M. Tatsumisago, S.-K. Lee, T. Minami, Y. Kowada, J. Non-Cryst. Solids 177 (1994) 154–163.
[10] A.R. West, Solid State Chemistry and its Applications, Chichester, UK, 1984, pp. 4–6.
[11] C.R. Feger, G.L. Schimek, J.W. Kolis, J. Solid State Chem. 143 (1999) 246–253.
[12] K.M. Ok, P.S. Halasyamani, Chem. Mater. 13 (2001) 4278–4284.
[13] (a) Y.G. Li, E.B. Wang, H. Zhang, G.Y. Luan, C.W. Hu, J. Solid State Chem. 163 (2002) 10–16;
(b) S.T. Wang, Y.G. Li, E.B. Wang, G.Y. Luan, C.W. Hu, N.H. Hu, H.Q. Jia, J. Solid State Chem. 167 (2002) 402–406;
(c) L. Xu, Y. Sun, E. Wang, E. Shen, Z. Liu, C. Hu, Y. Xing, Y. Lin, H. Jia, New J. Chem. 23 (1999) 1041–1044;
(d) M. Yuan, Y.G. Li, E.B. Wang, Y. Lu, CW. Hu, N.H. Hu, H.Q. Jia, J. Chem. Soc. Dalton Trans. (2002) 2916–2920;
(e) Y. Lu, E.B. Wang, M. Yuan, G.Y. Luan, Y.G. Li, J. Chem. Soc. Dalton Trans. (2002) 3029–3031;
(f) W.S. You, E.B. Wang, Y. Xu, Y.G. Li, L. Xu, C.W. Hu, Inorg. Chem. 40 (2001) 5471–5648;
(g) Y.G. Li, G.J.H. De, M. Yuan, E.B. Wang, R.D. Huang, C.W. Hu, N.H. Hu, H.Q. Jia, J. Chem. Soc. Dalton Trans. (2003) 331–334;
(h) Y.M. Chen, E.B. Wang, B.Z. Lin, S.T. Wang, J. Chem. Soc. Dalton Trans. (2003) 519–520;
(i) G.Y. Luan, Y.G. Li, S.T. Wang, E.B. Wang, Z.B. Han, C.W. Hu, N.H. Hu, H.Q. Jia, J. Chem. Soc. Dalton Trans. (2003) 233–235.
[14] V. Balraj, K. Vidyasagar, Inorg. Chem. 37 (1998) 4764–4774.
[15] V. Balraj, K. Vidyasagar, Inorg. Chem. 38 (1999) 1394–1400.
[16] V. Balraj, K. Vidyasagar, Inorg. Chem. 38 (1999) 3458–3462.
[17] V. Balraj, K. Vidyasagar, Inorg. Chem. 38 (1999) 5809–5813.
[18] R.A. Narayanan, Phys. Rev. B 64 (2001) 4207.
[19] J.C. McLaughlin, S.L. Tagg, J.W. Zwanziger, J. Phys. Chem. B 105 (2001) 67–75.
[20] M.G. Johnston, W.T.A. Harrison, J. Am. Chem. Soc. 124 (2002) 4576–4577.
[21] R.J. Gillsepie, Molecular Geometry, Van Norstand-Reinholdt, London, UK, 1972.
[22] (a) G.M. Sheldrick, SHELXS 97, Program for Crystal Structure Solution, University of Göttingen, 1997;
(b) G.M. Sheldrick, SHELXL 97, Program for Crystal Structure Refinement, University of Göttingen, 1997.
[23] D. Brown, D. Altermatt, Acta Cryst. B 41 (1985) 244–247.
[24] C.R. Becker, S.L. Tagg, J.C. Huffman, J.W. Zwanziger, Inorg. Chem. 36 (1997) 5559–5564.
[25] O. Lindqvist, Acta Chem. Scand. 26 (1972) 1423–1430.
[26] K. Hanke, V. Kupcik, O. Lindqvist, Acta Crystallogr. B 29 (1973) 963–970.